Tribology Transactions

ISSN: 1040-2004 (Print) 1547-397X (Online) Journal homepage: https://www.tandfonline.com/loi/utrb20

An Experimental Study on Film Thickness in a Rolling Bearing for Fresh and Mechanically Aged Lubricating Greases

Yuxin Zhou, Rob Bosman & Piet M. Lugt

To cite this article: Yuxin Zhou, Rob Bosman & Piet M. Lugt (2019) An Experimental Study on Film Thickness in a Rolling Bearing for Fresh and Mechanically Aged Lubricating Greases, Tribology Transactions, 62:4, 557-566, DOI: 10.1080/10402004.2018.1539202

To link to this article: https://doi.org/10.1080/10402004.2018.1539202

Accepted author version posted online: 29 Mar 2019.
Published online: 06 May 2019.

TRIBOLOGY TRANSACTIONS
2019, VOL. 62, NO. 4, 557–566
https://doi.org/10.1080/10402004.2018.1539202

An Experimental Study on Film Thickness in a Rolling Bearing for Fresh and Mechanically Aged Lubricating Greases

Yuxin Zhou[a], Rob Bosman[a], and Piet M. Lugt[a,b]

[a]Faculty of Engineering Technology, University of Twente, Enschede, The Netherlands; [b]SKF Research and Technology Development, Nieuwegein, The Netherlands

ABSTRACT

The lubricating film formation of greases has been widely studied using single contact ball-on-disc configurations. However, other than for oil, the film formation with grease is governed by starvation, which in a full bearing is clearly different from that of the single contact. In this paper, film thickness measurements for various greases in a shielded deep groove ball bearing will be presented. The results were obtained using an in-house-made film thickness measurement rig based on the 'electric capacitance method'. It will be shown that the film thickness may deviate from the theoretical elastohydrodynamic film thickness calculated from the base oil and that the film thickness is not constant in time. It will also be shown that the film thickness for longer times is not only determined by the classical properties such as oil viscosity and grease bleed but also by shear degradation of its microstructure.

ARTICLE HISTORY
Received 6 July 2018
Accepted 17 October 2018

KEYWORDS
Greases; grease application; ball bearings

Introduction

The performance of a bearing is strongly determined by the generated film thickness between the rolling elements and the raceway. If the film is insufficiently thick to separate the surfaces, direct contact occurs, leading to wear and/or a reduction of bearing life. The prediction of the lubricant film for grease lubrication is more difficult than for oil lubrication due to the rather complex lubrication mechanism given by starvation, replenishment, changes in lubricant properties (mechanical aging, oxidation, loss of bleeding property), etc., which is still not fully understood (Lugt *(1)*).

Extensive studies have been performed on grease lubrication using single contact configurations, where the rolling element-ring contacts inside a bearing are simulated in a ball-on-disc or disc-on-disc apparatus (Åström et al. *(2)*; Cann and Spikes *(3)*; Cann and Spikes *(4)*; Dyson and Wilson *(5)*; Poon *(6)*; Kageyama et al. *(7)*; Wen and Ying *(8)*). However, in this simplification many effects that have a major impact on film formation in a rolling bearing are ignored. Lubrication effects that cannot be adequately simulated by single contact tests include the large number of over-rollings, centrifugal forces, vibrations, cage scraping (Wikström and Jacobson *(9)*; Lugt *(10)*), as well as the slow change of the grease properties due to shear, oxidation and oil loss. Single contact measurements are very valuable but should ideally be combined with film thickness measurements in full bearings (Lugt *(1)*).

Mérieux et al. (Mérieux et al. *(11)*) gave four types of grease film thickness evolutions based on film thickness measurements in a single contact running at a constant speed: fully flooded; starved; starved with stabilization; starved with recovery. They particularly studied the fourth situation and attributed the film recovery to an increased lubricant availability due to grease shear degradation. The first condition was observed by Ward et al. (Ward et al. *(12)*) for a pair of axially loaded angular contact ball bearings fully packed with grease, where no significant film thickness decay was observed during 400h running. Continuous film thickness decrease was found when a reduced grease fill was used. The third condition was observed by Wilson (Wilson *(13)*) for a radially loaded roller bearing, which was attributed to temperature variation and partial starvation.

The film thickness for grease lubricated bearings is generally calculated using the base oil properties under fully flooded conditions (Cann and Lubrecht *(14)*). It was shown by Morales et al. (Morales-Espejel et al. *(15)*) and Dong et al. (Dong et al. *(16)*) that particularly under very low speeds, a large discrepancy occurs where a grease generates thicker films compared to that of the base oil, which is attributed to the thickener contribution and can be modeled with an 'effective viscosity' that is larger than the viscosity of the base oil (Cann and Lubrecht *(14)*).

Wikström & Jacobson (Wikström and Jacobson *(9)*) suggested a lubricant feed-loss mechanism for a grease lubricated roller bearing: the film thickness is given by a balance between the lubricant feed by grease bleeding, replenishment and drop feed from the roller adhered lubricant and the

CONTACT Yuxin Zhou y.zhou@utwente.nl
Color versions of one or more of the figures in the article can be found online at www.tandfonline.com/utrb.

Nomenclature

A_{Hertz} =	Hertzian contact area (m^2)	T =	Running temperature (°C)
$C_{bearing}$ =	The bearing capacitance (F)	R_q =	Arithmetical root mean square height deviation of an assessed profile (m)
C =	Bearing dynamic load rating (N)	R_x,R_y	Reduced contact radii (m)
C_i =	Capacitance formed by the ball and the inner ring (F)	$\bar{u}$ =	Mean entrainment speed of the contact surfaces (m/s)
C_o =	Capacitance formed by the ball and the outer ring (F)	$\bar{U}$ =	Speed parameter of the Hamrock-Dowson equation (-)
d_m =	Mean diameter (m)	V_{cap} =	Capacitance measuring instrument output voltage (V)
E' =	Reduced Young's Modulus (Pa)	W =	Load on each rolling element (N)
F_a =	Axial load (N)	$\bar{W}$ =	Load parameter in the Hamrock-Dowson equation (-)
$\bar{G}$ =	Material parameter in the Hamrock-Dowson equation (-)	Z =	Number of balls (-)
h =	Grease film thickness at the stable stage (m)	α =	Pressure-viscosity coefficient of the lubricating oil (Pa^{-1})
h_{grease} =	Calibrated grease film thickness (m)	η =	Lubricating oil viscosity ($Pa \cdot s$)
h_{oil} =	Calculated oil film thickness (m)	ε_0 =	Lubricant dielectric constant in vacuum (F/m)
L_{10} =	Estimated bearing life at which 10% of the bearing population has failed (h)	ε_r =	Lubricant dielectric constant in the contact area (F/m)
n =	Rotational speed of the bearing (rpm)		
P =	Equivalent bearing load (N)		

lubricant loss due to oxidation, polymerization, evaporation, surface spreading and drop loss. Cann & Lubrecht (Cann and Lubrecht *(17)*) suggested other replenishment mechanisms in a grease lubricated bearing: bulk grease migration due to ball spin, vibrations, cage effects and capillary reflow of the bled oil due to possible shock loads or machine start-stops.

Baker (Baker *(18)*) studied the influence of grease bleeding on bearing life. He concluded that a high bleed rate will prolong bearing life, but excessive bleeding (e.g. at high temperatures) will quickly 'dry-out' the grease and will therefore have a negative effect on the bearing life. Dalmaz & Nantua (Dalmaz and Nantua *(19)*) found that with an identical thickener, greases made of a higher base oil viscosity will increase the life of double row angular contact ball bearings. However, Ohno et al. (Ohno et al. *(20)*) observed that for thrust ball bearings, grease with higher base oil viscosity will aggravate starvation and therefore reduce the bearing life.

Albeit the grease film thickness observations mentioned above, there appears to be little published material on actual film thickness measurements in grease lubricated full bearings. In this paper film thickness measurements will be described in a deep groove ball bearing using an in-house-made film thickness measurement rig based on the electric capacitance method, a method earlier used in (Wikström and Jacobson *(9)*; Wilson *(13)*; Morales-Espejel et al. *(15)*; Ohno et al. *(20)*; Leenders and Houpert *(21)*; Jablonka et al. *(22)*; Wittek et al. *(23)*; Gatzen et al. *(24)*; Franke and Poll *(25)*).

Since the grease lubrication mechanism varies in time (churning phase, bleeding phase etc.) and is also known to be dynamic (Lugt *(1)*; Lugt et al. *(26)*), the grease films were measured during relatively long running time (100h). A comparison will be made between the measured grease film thickness and the theoretical fully flooded base oil film thickness calculated using the Hamrock and Dowson equation (Hamrock and Dowson *(27)*). In addition, to study the long-term behavior, the influence of grease shear degradation on the film thickness was studied by using mechanically aged greases.

Material and method

Sample preparation

The film thickness tests were first performed for six commercial lubricating greases, with different base oils and thickener materials/structures. To study the influence of grease shear degradation on the bearing film thickness, fresh polyurea grease (denoted as 'PU/E') was sheared inside an in-house-made 'Couette Aging Machine' with different aging levels (Zhou et al. *(28)*). Afterwards, the bearing film

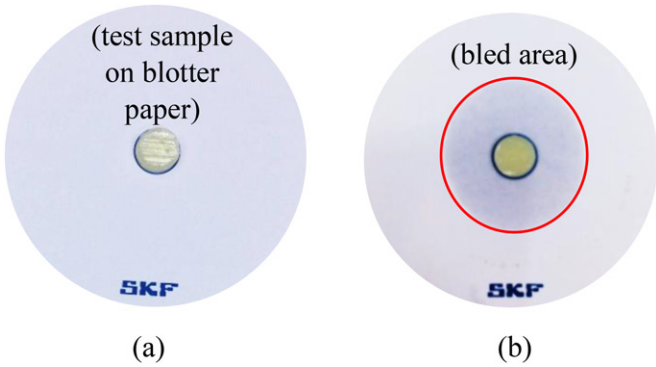

Figure 1. SKF grease bleed test: (a) Before the test; (b) After the test.

Table 1. Composition and properties of the tested greases

Fresh Grease	NLGI	Thickener type	Thickener concentration	Base oil type
CaS/PAO	1-2	Calcium sulfonate complex	26%	PAO
CaS/M	2	Calcium sulfonate complex	27%	Mineral oil
Li/M	3	Lithium	15%	Mineral oil
Li/SS	2	Lithium	17%	Mineral oil (semi-synthetic)
LiX/PAO	2-3	Lithium complex	20%	PAO
PU/E	2-3	Polyurea	26%	Ester

Table 2. Grease and oil properties

Grease sample	Grease bleed (mm^2)	Yield stress (Pa)	Kinematic viscosity at 40°C/100°C (cSt)	Kinematic viscosity at 60°C (cSt)	Pressure-viscosity coefficient α ($10^{-9}Pa^{-1}$)
Fresh CaS/PAO	269	106	320/30	121	17
Fresh CaS/M	115	154	420/26	131	27
Fresh Li/M	899	57	100/10	38	27
Fresh Li/SS	1357	35	42/7	21	24
Fresh LiX/PAO	479	54	191/42	106	17
Fresh PU/E	615	101	70/9	30	24

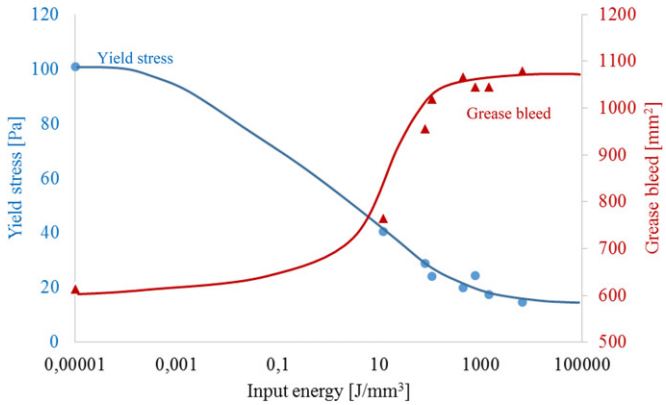

Figure 2. Condition of the PU/E samples plotted on a grease aging Master Curve for PU/E grease (Zhou et al. *(41)*) in combination with the grease bleed properties.

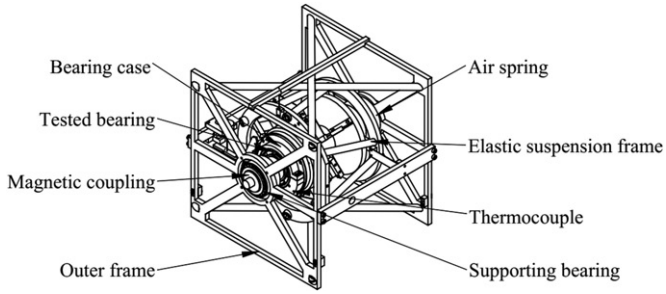

Figure 3. Bearing test rig.

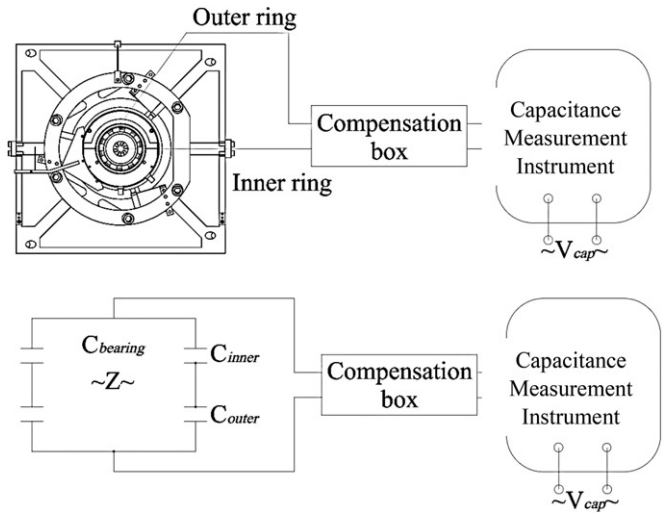

Figure 4. Film thickness measuring rig principle.

thickness was measured using the aged PU/E samples. The goal of this test was not only to study the impact of grease aging on film thickness but also to study the film formation of greases with the same chemical composition but different grease bleed, consistency and micro-structure. Detailed information on the grease composition is shown in Table 1.

Sample characterization

As mentioned above, grease bleeding is considered to be a major property determining the film thickness. Large volumes of grease are required for measuring grease bleed using the standardized methods such as DIN 51817/IP 121 (Lugt *(1)*). In this work, grease bleed was measured using the SKF Grease Test Kit (Noordover et al. *(29)*), which only uses 125.6 mm^3 of grease. As shown in Fig. 1a, the grease sample was positioned in the center of a piece of blotter paper. The tested sample is heated on a heater in the open air at 60°C for two hours. During this time, the base oil spreads through the paper forming an 'oil stain'. Next, the surface area of the oil stain is measured with unit mm^2, which is a measure for the grease bleed rate. For each grease sample, the test was performed at least twice, and the repeatability is better than 90%.

In addition to grease bleeding, the grease rheology was measured. There are numerous rheological parameters that can be measured but in this study the yield stress is considered, which is the most important parameter related to the mobility of the grease. Here the grease yield stress was obtained from the rheological oscillatory strain sweep measurements at 25°C, following the method proposed by Cyriac et al. (Cyriac et al. *(30)*). For every tested sample, at least two measurements were performed and the measuring spread was less than 10%. The average values for grease bleed and yield stress are shown in Table 2. The fully flooded base oil film thickness was calculated using the pressure-viscosity coefficient of the bled oil (calculated by minimizing the error between the ball-on-disc film thickness and the calculated Hamrock and Dowson film thickness (Hamrock and Dowson *(27)*) following Van Leeuwen's method (Cyriac et al. *(31)*; Van Leeuwen *(32)*). Grease bleed is closely related to the base oil viscosity (Lugt *(1)*). Therefore, the base oil viscosity was calculated, using Walther equation (Walther *(33)*), at the same temperature at which the bleeding tests (60°C) were done. The values are provided in Table 2.

To indicate the aging level of the sheared PU/E, the changes of grease bleed and yield stress are plotted versus the input aging energy in Fig. 2. This figure shows that the samples that are used here reflect the full spectrum of shear degradation.

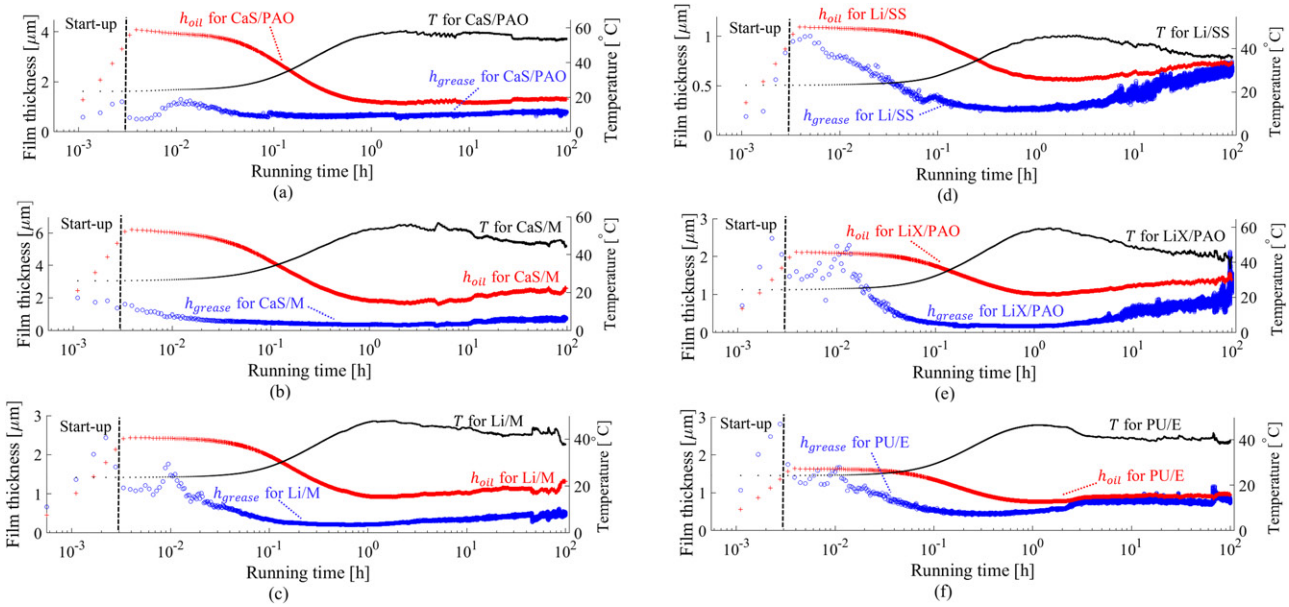

Figure 5. Film thickness profile of CaS/PAO (a); CaS/M (b); Li/M (c); Li/SS (d); LiX/PAO (e); PU/E (f).

After the test, the grease was collected from the bearing shields and in the vicinity of the running track. The absence of oxidation was confirmed using Fourier-Transform Infra-Red spectroscopy (results not shown).

Film thickness measuring rig

In this paper, the grease film thickness evolution in a full deep groove ball bearing 6209-2Z/C3 was studied with inner ring rotation. The bearing test rig is shown in Fig. 3. The outer ring of the tested bearing was clamped inside the bearing case which was in turn bolted to a frame with elastic hinges. The bearing inner ring was driven via the shaft by an electric motor (not shown in Fig. 3) through a magnetic coupling. To ensure a proper alignment, the shaft was supported by a tapered roller bearing mounted to the outer frame.

To obtain a uniform pressure distribution and film thickness for each rolling element, a pure axial load F_a was applied. The load was set as $\frac{C}{P} = 40$, giving an axial load of $F_a = 513\ N$. The speed was $n = 2500$ rpm corresponding to $ndm = 162500\ \mathrm{mm}/min$ (product of speed and mean diameter), which is relatively low but in the same order as used in standard test rigs such as the R0F + grease life test (Lugt et al. *(34)*). The tests were run for 100h using six different fresh greases (Table 1) to ensure that the grease will undergo all relevant phases. In addition, 10h tests (which was sufficiently long to reach a steady state film) were carried out for the aged PU/E greases.

The bearing was run at room temperature and the self-induced temperature was recorded by a thermocouple attached to the bearing outer ring through a hole in the bearing case. In addition, the applied load was calculated from the air pressure of the air spring. For each test, 30% of the bearing free volume was filled with the grease sample from both sides. Afterwards, the bearing was closed by the shields. Before and after each test, the bearing was weighted to measure possible leakage.

The bearing film thickness was obtained using a commercial Capacitance Measuring Instrument (Heemskerk et al. *(35)*), by measuring the capacitance of the bearing $C_{bearing}$, which was treated as the sum of Z capacitors in parallel, each one determined by the lubricant film between the inner ring-ball (C_i) and ball-outer ring (C_o) (Z is the number of

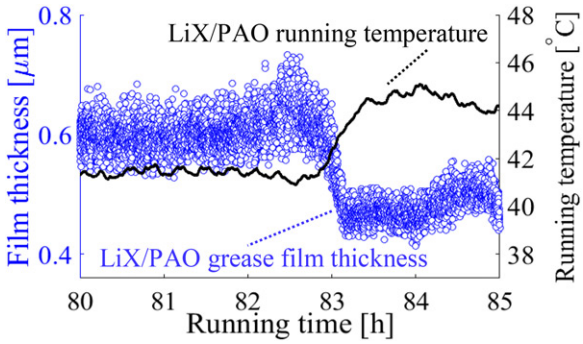

Figure 6. LiX/PAO film thickness event (zoom-in from Fig. 5e).

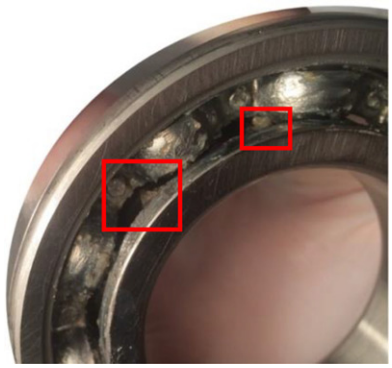

Figure 7. Grease lumps observed on the running track after 100h running for LiX/PAO.

the balls). Figure 4 shows the basic principle of the film thickness measuring rig. The bearing inner ring was connected to the Capacitance Measuring Instrument via a mercury contact attached to the rotating shaft. The stationary bearing outer ring was connected to the Capacitance Measuring Instrument directly. The rotor and stator were electrically isolated by the lubricant film. A compensation box (with capacitors) was connected in-between to compensate the inductance of the connecting leads. The Capacitance Measuring Instrument output voltage V_{cap} can be considered as a measure for the average of the inner and outer ring film thickness. To transfer V_{cap} to the bearing film thickness, a calibration was performed using Wilson's method (Wilson *(13)*) but using the bled oil under the same running conditions as in the grease film thickness measurements, for details see the Appendix.

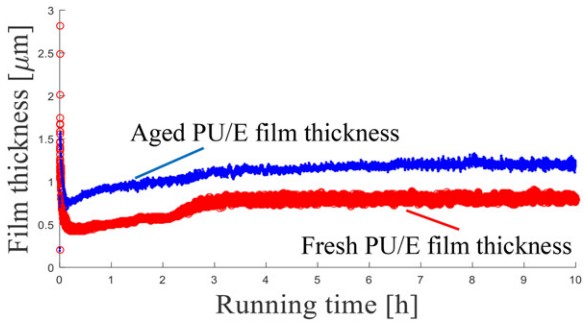

Figure 8. Film thickness profiles for fresh and aged PU/E.

Film thickness for fresh greases

Overall film thickness profile

The grease film thickness h_{grease} results obtained from the 100h continuous running tests are presented in Fig. 5. Note that the bearing is starting up in approximately the first $5 \sim 10$ seconds (2×10^{-3} hours). It is only after this time that the speed is constant. Figure 5 also shows the running temperature T and the predicted fully flooded film thickness according to the Hamrock and Dowson equation (Hamrock and Dowson *(27)*), denoted by 'oil film thickness' h_{oil}:

$$\frac{h_{oil}}{R_y} = 2.69 \times 10^9 \overline{U}^{0.67} \overline{G}^{0.53} \overline{W}^{-0.067} \left(1-0.61e^{-0.75\left(\frac{R_x}{R_y}\right)^{0.64}}\right), \tag{1}$$

with

$$\overline{U} = \frac{\overline{u}\cdot\eta}{E'\cdot R_y}, \quad \overline{G} = \alpha \cdot E', \quad \overline{W} = \frac{W}{E'\cdot {R_y}^2}. \tag{2}$$

Here h_{oil} is the calculated EHL film thickness; $\overline{u}$ is the mean entrainment speed calculated from the bearing kinematics assuming pure rolling (Harris *(36)*); η is the temperature dependent base oil viscosity calculated using the Walther equation (Walther *(33)*); α is the bled oil pressure-viscosity coefficient; E' is the reduced Young's Modulus of the contact material; R_x, R_y are the reduced radii of the contact; W is the load for each rolling element.

The viscosity in this equation is calculated using the base oil viscosity at the measured bearing temperature. The

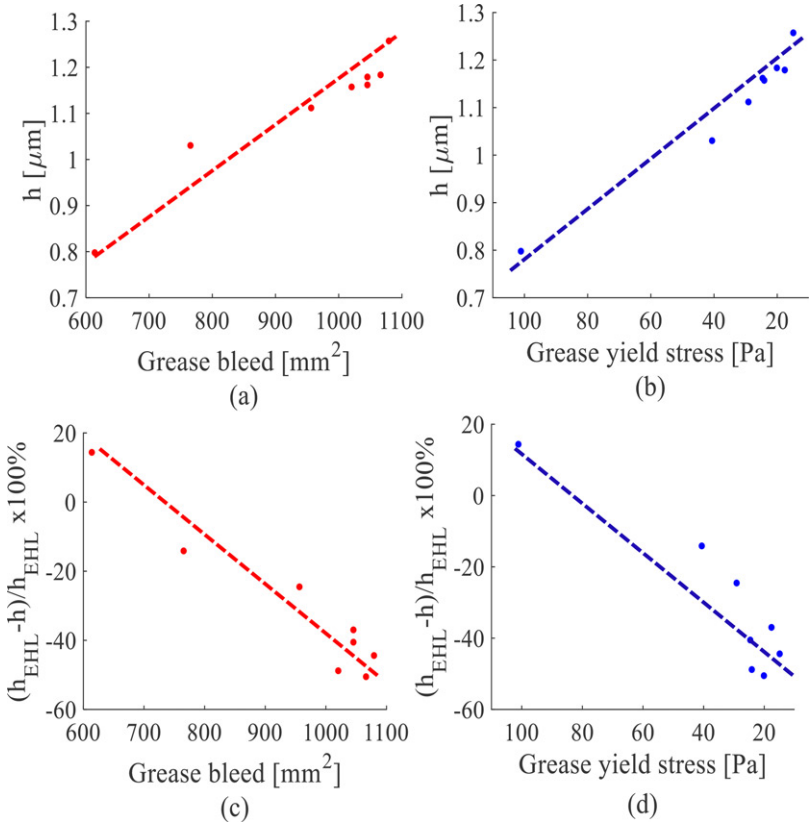

Figure 9. Film thickness results for fresh and aged PU/E vs grease bleed (a, c) and yield stress (b, d) after 5 hours running.

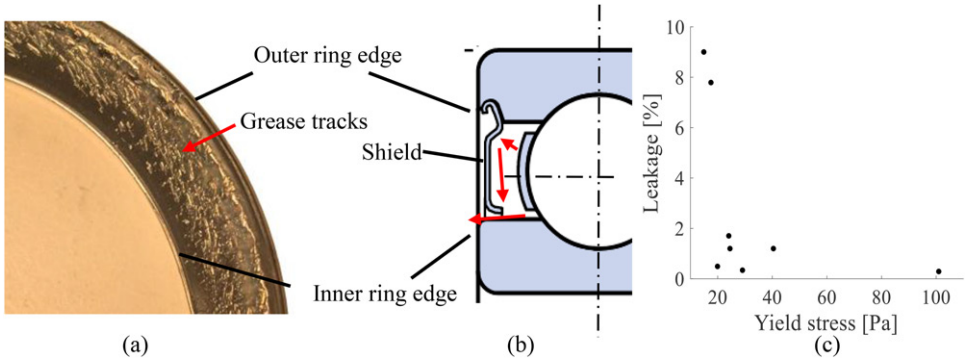

Figure 10. Bearing leakage study: (a) grease track on the shield inner surface, (b) schematic drawing of the grease flow inside a shielded bearing, (c) PU/E grease leakage vs shear degradation.

speeds and loads are constant. Hence, a variation in h_{oil} is only caused by a variation in temperature.

After starting up, the large grease film thickness suggests the occurrence of fully flooded conditions. For a freshly greased bearing, after starting up, there will be much bulk grease in the inlet of the contacts, which will be fully flooded with grease and not only oil. The film thickness will be approximately equal to the predicted oil film thickness (see also Cousseau et al. (Cousseau et al. *(37)*).

The initial large grease film is followed by a sharp decrease. Wilson (Wilson *(13)*) attributed such a fast decrease to the rising temperature resulting in a lower viscosity. However, the grease film thickness decrease is more pronounced compared to the calculated temperature dependent oil film thickness. This is ascribed to starvation: the subsequent decrease of the grease film thickness is a result of progressive grease channeling and migration due to side-flow (Ward et al. *(12)*). This will ultimately result in a reduced availability of lubricant at the inlet area leading to a decreasing film thickness.

Figure 5 shows three greases (Li/SS in Fig. 5d, LiX/PAO in Fig. 5e and PU/E in Fig. 5f) for which the film thickness is initially equal to the oil film thickness, after which it deviates from this, but ultimately approaches the oil film thickness again in the bleeding phase. For Li/SS this can be ascribed to a high grease bleed (see Table 2). For LiX/PAO this can be attributed to a micro-churning induced event as explained in the next section. For PU/E this can be ascribed to shear degradation in the churning phase (Lugt *(1)*; Wilson *(13)*). This shear degradation will contribute to the mobility of the grease (Cann and Lubrecht *(38)*). It was shown in (Zhou et al. *(28)*) that PU/E is an aging sensitive grease (low shear stability). Albeit its relatively low bleeding rate, a good film recovery can be observed after the churning phase (Fig. 5f). More details about the influence of aging on PU/E film thickness will be presented later. The film thickness measurements with CaS/M and CaS/PAO, however, show severe starvation (Fig. 5a and b), which can be ascribed to the combination of a low grease bleed and high shear stability. These observations are in line with the ball-on-disc measurements of Mérieux et al. (Mérieux et al. *(11)*) who also noted that a grease with a poor shear stability shows a film thickness recovery after an initial decay whilst

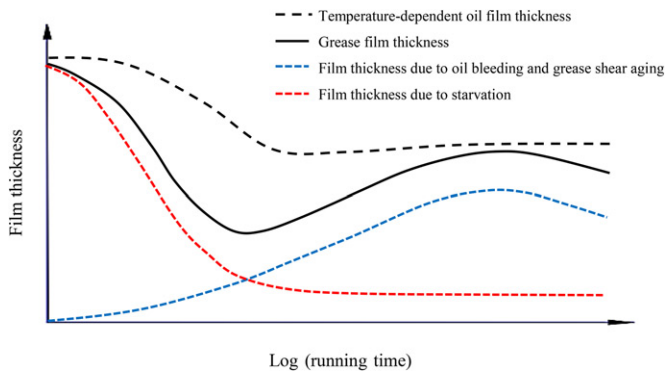

Figure 11. Grease film thickness variation inside a rolling bearing.

a shear stable grease shows continuous starvation without recovery.

To conclude, in the initial phase the film thickness may decrease sharply followed by recovery (a first 'event' in the film thickness). This is determined by the rates of starvation and lubricant feed, which again is determined by grease bleed and shear stability. When a 'feed and loss' balance is reached (Wikström and Jacobson *(9)*), the grease film thickness levels out at a more-or-less stable value. After the initial decay, no considerable grease film decreasing trend was observed during the 100 hours' running. Obviously, this time may be long for a test but is extremely short compared to the expected long grease life at this relatively low running temperature, load and speed, e.g. $L_{10} = 50\ 000$ hours.

Film thickness events during the stable stage

It is noteworthy that for LiX/PAO (Fig. 5e), PU/E (Fig. 5f) and Li/M (Fig. 5c), film thickness events are observed, coming back occasionally during the equilibrium stage. Such film thickness fluctuations were earlier observed by Lugt et al. in (Lugt et al. *(26)*). They ascribed this dynamic behavior to a decrease in film thickness due to starvation until metal-to-metal contact occurs causing heat development, softening of grease or increase in grease bleed resulting in replenishment and a thicker film again. However, this does not occur here. The film thickness perturbations take place in a situation where the film thickness is sufficiently thick to separate the two contacting surfaces: for LiX/PAO the equilibrium film thickness was 0.8 μm, for PU/E 0.8 μm and for

Li/M 0.44 μm. This is much larger than the roughness of the combined surfaces of the bearing which is about $R_q = 0.07$ μm.

One of the grease film events for LiX/PAO is plotted in Fig. 6. Clearly, a similar film thickness increment took place as in the event immediately after starting up. An increase in film thickness just before the event seems to happen almost simultaneously with an increase in temperature. Similar event behavior was observed for the PU/E and Li/M.

This phenomenon can be ascribed to churning. During running, a fraction of the grease from the reservoirs may incidentally fall back into the contact area because of creep flow, vibrations, centrifugal force and/or cage scraping (Wilson *(13)*; Cann and Lubrecht *(14)*; Lugt et al. *(26)*; Cann and Lubrecht *(39)*). The resulting (micro-)churning will lead to the generation of extra frictional heat (Fig. 6). The introduction of bulk grease into the contact area will generate a thicker film, which subsequently drops rapidly due to an increase in temperature, followed by a slow recovery due to a temperature reduction, again caused by side flow and starvation. As shown in Fig. 5e, LiX/PAO was experiencing severe film thickness fluctuations at the end of the 100h running test. Once the test was finished, some remaining grease lumps were observed on the running track of the bearing, see Fig. 7. This agrees with the (micro-) churning induced film thickness fluctuation as mentioned above.

Film thickness for mechanically aged grease

In this section, film thickness results will be presented for both fresh and aged PU/E grease. As shown in Fig. 2, mechanical degradation of this polyurea grease does not only lead to softening but also results in an increase of grease bleeding. The change of grease properties will result in a change film build-up capability as shown in Fig. 8. The film thickness results for PU/E at different aging levels are summarized in Fig. 9, where the grease film thickness h (average measured film thickness after 5 hours until 10 hours running time) and the degree of grease starvation $\frac{h_{oil}-h}{h_{oil}} \times 100\%$ are plotted for fresh and aged PU/E versus oil bleed and yield stress.

The results show that the grease film thickness increases with increased aging (so with increasing grease bleeding and decreasing yield stress). In addition, all of the aged PU/E samples generate thicker films compared to the predicted oil film thickness ($\frac{h_{oil}-h}{h_{oil}} < 0$). As the grease aging continues, the progressively destroyed thickener network is no longer capable to hold oil, which increases the availability of free oil for replenishment (higher oil bleed) and thereby reduces starvation, see Fig. 9a and c. In addition, the resulting grease softening will again promote grease migration inside the bearing: it will be easier for the aged grease (with lower yield stress) to replenish the bearing raceway (Kaneta et al. *(40)*), see Fig. 9b and d. Ultimately, in the case of severe degradation, the original thickener material will be sheared into small fragments (a later paper will cover the change of PU/E micro-structure in more detail). The grease has softened so much that the reservoirs are no longer stable and the thickener particles will enter the inlet of the contacts. According to the empirical model presented by Cyriac et al. (Cyriac et al. *(31)*), an increase of 40% film thickness would be caused by a reduction of the thickener length by a factor of 4. This agrees with the change of grease thickener micro-structure observed during the aging process (Zhou et al. *(41)*). Therefore, grease shear degradation contributes in three ways to a reduction of starvation: higher grease bleeding, more migration and the formation of smaller thickener particles which enter the contact area easier.

Leakage study

It is well known that the film thickness decreases versus time (Lugt *(1)*). This decrease ultimately leads to the end of grease life. The film thickness measurements of the aged grease, however, suggest that with increased aging, the film would only become thicker, which is contradicting field observations. It is expected that starvation will ultimately occur again, because of leakage, oxidation, polymerization or evaporation. Since the temperatures are low in the current study, leakage is the most probable cause. During the aged-PU/E film thickness measurements, leakage was indeed observed by the grease accumulation around the gap between the shield and the inner ring.

According to Hiraoka (Hiraoka *(42)*), grease leakage is caused by three factors: centrifugal force, grease flow due to shear softening or high temperature and the pushing-out force generated by the rolling motion. Immediately after starting up, the centrifugal force will overcome the grease yield stress and the adhesive force, throwing the grease to the bearing periphery. Once the grease reaches the outer ring edge, for a shielded bearing, it can be expected that the accumulated grease at the outer ring inner diameter will push the grease towards inner ring over the shield surface, see the grease track in Fig. 10a. The grease will then flow/leak though the non-contacting shield, an effect that may be enhanced by the elastic properties of the grease (Baart et al. *(43)*) (Fig. 10b). Grease leakage versus yield stress is presented in Fig. 10c. This graph shows that softening due to aging facilitates the grease flow inside the bearing and results in higher leakage. This will again result in a reduction of the grease reservoir inside the bearing, thus reduce the lubricant feed to the contacts and ultimately will lead to starvation and a decrease of the grease film thickness.

To summarize, grease aging will contribute to an increase in film thickness due to thickener breakdown leading to softening and increased grease bleed resulting in less or no starvation. In addition, it will lead to a reduced thickener fiber length which will cause an increased thickener particle entrainment in the contacts and further increase of the film thickness. However, this decay in grease consistency and increase of grease bleeding will also result in leakage and a drain of the grease reservoir, which will ultimately reduce the film thickness again. In the 100h running tests the initial 30% grease filling is sufficient to feed the contacts such that no film thickness decreasing trend was observed after the

initial event. For future work, it is recommended to perform measurements with reduced filling of aged grease to verify the grease leakage effect on bearing film thickness.

Discussion

In this study, the measured grease film thickness inside an axially loaded deep groove ball bearing has been compared with the fully flooded ElastoHydrodynamicLubrication (EHL) film thickness of the base oil at the self-induced running temperature.

All greases, except for the CaS greases initially show fully flooded films similar to the films that would be formed by base oil. The severe starvation already in the startup phase of the CaS greases is caused by the high yield stress in combination with very low grease bleed. The results show that the grease film thickness was quite constant for the CaS greases but not for the other greases; after starting-up, a fully flooded condition occurs, where grease is functioning as the lubricant. The grease channeling results in a rapid decrease of the film thickness, which is even further decreased by an increasing temperature. In the meantime, the grease reservoir starts bleeding oil. The grease shear degradation in the contacts and in the vicinity of the contacts in combination with an increased temperature will promote this grease bleed. Shear degradation will also lead to grease softening, which again facilitates replenishment. This results in an increase of the film thickness up to a relatively stable value, when the feed-and-loss mechanisms are in balance. After this, during the approximately stable stage, film thickness fluctuations are observed. This is attributed to an incidental release of bulk grease towards the contact areas due to vibrations, creep flow, centrifugal forces or cage scraping. Meanwhile, grease shear degradation will reduce the length of the grease fibers generating smaller particles, which are more easily entrained into the contacts than the long fibers ultimately leading to thick(er) films. However, this softening of the grease will also result in leakage and a drain of the grease reservoir. It is expected that this will lead to thinner films after long running times (compared to the running times in the current study).

Figure 11 schematically shows the film thickness evolution for greases with a fibrous microstructure, which were found to be aging sensitive (Zhou et al. *(28)*). The grease film thickness (black line) is the sum of the film thickness related to starvation (red dotted line) and the film thickness due to grease bleed and shear aging (blue dotted line). Initially the film thickness is equal to that of the fully flooded oil film thickness. After which, almost immediately starvation occurs. This would lead to a film collapse if the contacts would not be fed by bled oil. A minimum film thickness occurs at the crossing point where the further decrease of film thickness is stopped by sufficient oil bleed. After this the film will grow until a balance of feed and loss of lubricant to the contact takes place. After much longer times the films will again decrease by leakage, oxidation, evaporation etc., where the dominating loss mechanism will be given by the operating conditions, for example at high temperatures this will be oxidation.

The CaS greases show a low grease bleed and high yield stress. They are very shear stable and will therefore maintain a low oil bleed and high yield stress throughout the test. The behavior outlined in Fig. 11 therefore does not apply to this grease type. This does not mean that these greases would not perform well in a rolling bearing. The calcite in these greases makes a viscous deposit of calcium carbonate (Giasson et al. *(44)*), providing physically and chemically adsorbed layer (Liu et al. *(45)*) with very good boundary lubrication properties.

Conclusions

This study shows that the classic fully flooded EHL theory cannot directly be applied to the film thickness estimations of grease lubricated bearings. The lubrication mechanism is governed by starvation. This would lead to very thin films but will be compensated by oil bleed and by the entrainment of thickener particles. Both effects are enhanced by shear degradation which will cause an increase of grease bleed and decrease of the thickener particle length. This will also lead to a reduction of the yield stress which will enhance the mobility of the grease. However, shear degradation will also have negative effects for the performance of rolling bearings, which however, is outside the scope of this paper.

The CaS greases show a different lubrication mechanism. For these greases thin hydrodynamic films were found here caused by a low oil bleed and the absence of shear degradation.

All film thickness measurements showed a dynamic behavior. In addition to the first event after startup, also after longer times film thickness fluctuations were found. This behavior was reported earlier in cylindrical roller bearings running at relatively high speeds and was causes by film breakdown leading to (local) heat development (Lugt et al. *(26)*). Under these relatively mild conditions these 'events' were likely to be caused by the release of grease lumps leading to (micro-) churning and heat development.

Acknowledgement

The authors would like to thank SKF Research and Technology Development for technical and financial support.

References

(1) Lugt, P.M. (2013), *Grease Lubrication in Rolling Bearings*, Hoboken, NJ: John Wiley and Sons.

(2) Åström, H., Isaksson, O., and Höglund, E. (1991), "Video Recordings of an EHD Point Contact Lubricated With Grease," *Tribology International*, **24**(3), pp 179–184.

(3) Cann, P. and Spikes, H. (1992), "Fourier-Transform Infrared Study of the Behavior of Grease in Lubricated Contacts," *Lubrication Engineering (United States)*, **48**.

(4) Cann P. and Spikes, H. (1992), "Film Thickness Measurements of Lubricating Greases Under Normally Starved Conditions," *NLGI spokesman*, **56**(2), pp 21–27.

(5) Dyson, A. and Wilson, A.R. (1969), "Film Thicknesses in Elastohydrodynamic Lubrication of Rollers by Greases," *Proceedings of the Institution of Mechanical Engineers, Conference Proceedings*, London, England: SAGE Publications Sage UK.

(6) Poon, S. (1972), An Experimental Study of Grease in Elastohydrodynamic Lubrication," *Journal of Lubrication Technology*, **94**(1), pp 27–34.

(7) Kageyama, H., Machidori, W., and Moriuchi, T. (1984), "Grease Lubrication in Elastohydrodynamic Contacts," *NLGI Spokesman*, **48**(3), pp 72–81.

(8) Wen, S.Z. and Ying, T.N. (1988), "A Theoretical and Experimental Study of EHL Lubricated With Grease," *Journal of tribology*, **110**(1), pp 38–43.

(9) Wikström, V. and Jacobson, B. (1997), "Loss of Lubricant from Oil-Lubricated Near-Starved Spherical Roller Bearings," *Proceedings of the Institution of Mechanical Engineers, Part J*, **211**(1), pp 51–66.

(10) Lugt, P.M. (2009), "A review on Grease Lubrication in Rolling Bearings," *Tribology Transaction*, **52**(4), pp 470–480.

(11) Mérieux, J., Hurley, S., Lubrecht, A., and Cann P. (2000), "Shear-Degradation of Grease and Base Oil Availability in Starved EHL Lubrication," *Tribology Series*, **38**, pp 581–588.

(12) Ward, P., Leveille, A., and Frantz, P. (2008), "Measuring the EHD Film Thickness in a Rotating Ball Bearing," *39th Aerospace Mechanisms Symposium*.

(13) Wilson, A. (1979), "The Relative Thickness of Grease and Oil Films in Rolling Bearings," *Proceedings of the Institution of Mechanical Engineers*, **193**(1), pp 185–192.

(14) Cann, P. and Lubrecht, A. (1999), "An Analysis of the Mechanisms of Grease Lubrication in Rolling Element Bearings," *Lubrication Science*, **11**(3), pp 227–245.

(15) Morales-Espejel, G., Lugt, P.M., Pasaribu, H.R., and Cen, H. (2014), "Film Thickness in Grease Lubricated Slow Rotating Rolling Bearings," *Tribology International*, **74**, pp 7–19.

(16) Dong, D., Komoriya, T., Endo, T., and Kimura, Y. (2011), "Monitoring Lubrication Conditions with Grease in Ball Bearings. *International Tribology Conference*.

(17) Cann, P. and Lubrecht, A. (2003), "The Effect of Transient Loading on Contact Replenishment with Lubricating Greases," *Tribology Series: Elsevier*, **43**, pp 745–750.

(18) Baker, A. (1958), "Grease bleeding—a Factor in Ball Bearing Performance," *NLGI Spokesman*, **22**(9), pp 271–277.

(19) Dalmaz, G. and Nantua, R. (1987), "An Evaluation of Grease Behavior in Rolling Bearing Contacts," *Lubrication Engineering*, **43**(12), pp 905–915.

(20) Ohno, N., Tanimoto, K., Kuwano, N., and Hirano, F. (1998), "Effect of the Base Oil Viscosity of Lithium Soap Greases on Life of Thrust Ball Bearings," *Japanese Journal of Tribology*, **43**(12), pp 1545–1556.

(21) Leenders, P. and Houpert, L. (1987), "Paper XXI(i) Study of the Lubricant Film in Rolling Bearings; Effects of Roughness," *Tribology Series*, **11**(Supplement C), pp 629–638.

(22) Jablonka, K., Glovnea, R., and Bongaerts, J. (2018), "Quantitative Measurements of Film Thickness in a Radially Loaded Deep-Groove Ball Bearing," *Tribology International*, **119**, pp 239–249.

(23) Wittek, E., Kriese, M., Tischmacher, H., Gattermann, S., Ponick, B., and Poll, G. (2010), "Capacitances and Lubricant Film Thicknesses of Motor Bearings Under Different Operating Conditions," *Electrical Machines (ICEM), 2010 XIX International Conference on: IEEE*.

(24) Gatzen, M., Pape, F., Bruening, C., Gatzen, H., Arlinghaus, H., and Poll, G. (2010), "Correlation Between Performance and Boundary Layers in High Speed Bearings Lubricated with Polymer-Enhanced Greases," *Tribology International*, **43**(5), pp 981–989.

(25) Franke, E. and Poll, G. (1999), "Service Life and Lubrication Conditions of Different Grease Types in High-Speed Rolling Bearings," *Tribology Series*, **36**, pp 601–609.

(26) Lugt, P.M., Velickov, S., and Tripp, J.H. (2009), "On the Chaotic Behavior of Grease Lubrication in Rolling Bearings," *Tribology Transaction*, **52**(5), pp 581–590.

(27) Hamrock, B.J. and Dowson, D. (1978), "Elastohydrodynamic Lubrication of Elliptical Contacts for Materials of Low Elastic Modulus. I: Fully Flooded Conjunction," *ASME Journal of Lubrication Technology*, **100**(2), pp 236–245.

(28) Zhou, Y., Bosman, R., and Lugt P.M. (2018), "A Master Curve for the Shear Degradation of Lubricating Greases with a Fibrous Structure," *Tribology Transactions*, **6**(just-accepted), pp 1–21.

(29) Noordover, A., David, S., Fiddelaers, F., Van Den Kommer, A., inventors. (2016), AnonymousGrease Test Kit and Methods of Testing Grease.

(30) Cyriac, F., Lugt, P.M., and Bosman, R. (2015), "On a New Method to Determine the Yield Stress in Lubricating Grease," *Tribology Transaction*, **58**(6), pp 1021–1030.

(31) Cyriac, F., Lugt, P., Bosman, R., Padberg, C., and Venner C. (2016), "Effect of Thickener Particle Geometry and Concentration on the Grease EHL Film Thickness at Medium Speeds," *Tribology Letters*, **61**(2), pp 1–13.

(32) Van Leeuwen, H. (2009), "The Determination of the Pressure—Viscosity Coefficient of a Lubricant through an Accurate Film Thickness Formula and Accurate Film Thickness Measurements," *Proceedings of the Institution of Mechanical Engineers, Part J: Journal of Engineering Tribology*, **223**(8), pp 1143–1163.

(33) Walther, C. (1931), "The Evaluation of Viscosity Data," *Erdol und Teer*, **7**, pp 382–384.

(34) Lugt, P.M., Kommer, A., Lindgren, H., and Deinhofer, L. (2013), "The ROF Methodology for Grease Life Testing," *NLGI Spokesman*, **77**(1), pp 18–27.

(35) Heemskerk, R., Vermeiren, K., and Dolfsma, H. (1982), "Measurement of Lubrication Condition in Rolling Element Bearings," *ASLE Transactions*, **25**(4), pp 519–527.

(36) Harris, T.A. (2001), Rolling Bearing Analysis, Hoboken, NJ: John Wiley and Sons.

(37) Cousseau, T., Graça, B., Campos, A., and Seabra, J. (2015), "Grease Aging Effects on Film Formation Under Fully-Flooded and Starved Lubrication," *Lubricants*, **3**(2), pp 197–221.

(38) Cann, P. and Lubrecht, A. (2007), "Bearing Performance Limits with Grease Lubrication: The Interaction of Bearing Design, Operating Conditions and Grease Properties," *Journal of Physics D: Applied Physics*, **40**(18), p 5446.

(39) Cann, P. and Lubrecht, A. (2005), "Bearing Performance Limits with Grease Lubrication," *World Tribology Congress III: American Society of Mechanical Engineers*, pp 35–36.

(40) Kaneta, M., Ogata, T., Takubo, Y, and Naka, M. (2000), "Effects of a Thickener Structure on Grease Elastohydrodynamic Lubrication Films," *Proceedings of the Institution of Mechanical Engineers, Part J: Journal of Engineering Tribology*, **214**, pp 327–336.

(41) Zhou, Y., Bosman, R., and Lugt, P.M. (2016), "A Model for Shear Degradation of Lithium Soap Grease at Ambient Temperature," *Tribology Transaction*, **12/21**, pp 1–10.

(42) Hiraoka, N. (2012), "On Grease Leakage from Rolling Bearings," *Tribology International*, **50**, pp 45–50.

(43) Baart, P., Lugt, P.M., and Prakash, B. (2014), "On the Normal Stress Effect in Grease-Lubricated Bearing Seals," *Tribology Transaction*, **57**(5), pp 939–943.

(44) Giasson, S., Espinat, D., and Palermo, T. (1993), "Study of Microstructural Transformation of Overbased Calcium Sulphonates During Friction," *Lubrication Science*, **5**(2), pp 91–111.

(45) Liu, D., Zhao, G., and Wang, X. (2012), "Tribological Performance of Lubricating Greases Based on Calcium Carbonate Polymorphs Under the Boundary Lubrication Condition," *Tribology Letters*, **47**(2), pp 183–194.

(46) Bader, N., Furtmann, A., Tischmacher, H., and Poll, G. (2017), "Capacitances and Lubricant Film Thicknesses of Grease and Oil Lubricated Bearings," *STLE Annual Meeting & Exhibition*.

Appendix-film thickness calibration

In an axially loaded ball bearing, the films separating the balls from the rings are assumed to be long, thin and uniform. The rolling contacts can then be regarded as capacitor plates with the lubricant as the insulating medium. The thickness of the lubricant film is then equal to the distance between the capacitor plates. The film thickness can therefore be calculated using (Jablonka et al. *(22)*; Franke and Poll *(25)*):

$$h_{bearing} = \varepsilon_0 \cdot \varepsilon_r \cdot \frac{A_{Hertz}}{C_{bearing}},$$

where ε_0 is the lubricant dielectric constant in vacuum, ε_r is the lubricant dielectric constant in the contact area, A_{Hertz} is the total Hertzian contact area, $C_{bearing}$ is the bearing capacitance and $h_{bearing}$ is the average film thickness. It is complex to calculate the film thickness from this equation: firstly, the redundant capacitance at the inlet and outlet contact region will make it difficult to separate the capacitance at the Hertz contact area from the total bearing capacitance; secondly, the dielectric constants ε_0 and ε_r for the tested lubricant are unknown. This was avoided by determining the grease film thickness directly by calibrating the Capacitance Measuring Instrument signal V_{cap} using the grease bled oils. It is assumed that, at these medium speed, most of the lubricant inside the contacts consists of bled oil. In addition, it may be assumed that grease and bled oil under shear have similar dielectric constants (10% difference as shown by Wilson (Wilson *(13)*)). Hence, an identical film thickness for both grease and its bled oil at the same running conditions will give a similar measured capacitance (Capacitance Measuring Instrument signal V_{cap}). It was also assumed that the inlet and outlet of the contacts do not significantly contribute to the capacitance difference between the bled oil calibration and the grease film measurements. For the grease lubricated bearing this will only play some role in the case of severe starvation.

The bled oil was extracted from the tested grease sample using a centrifuge. The FTIR spectra comparison confirmed that there was no thickener material in the bled oil; in addition, the viscosity difference between the base oil and bled oil for these greases is negligible (Cyriac et al. *(31)*). The contact size and dielectric properties are pressure dependent (Bader et al. *(46)*). Therefore, the same load (axial force) was applied for the calibrating tests as for the grease film thickness measurements. The calibrating tests were performed using the same bearing but open (without shield) at 25°C.

By doing a series of speed sweep calibrating tests under fully flooded conditions, the recorded Capacitance Measuring Instrument signal V_{cap} was related to the calculated bled oil film thickness based on the Hamrock and Dowson equation. During calibration, oil was fed occasionally to the contact areas using a syringe and no significant V_{cap} fluctuations were observed. This confirmed that he calibrating tests were running in fully flooded conditions (Wilson *(13)*) and that the Hamrock and Dowson equation is applicable. For each bled oil, calibration curve was made between the calculated film thickness and V_{cap}.